J. Phys. B: At. Mol. Opt. Phys. **33** (2000) L209–L213. Printed in the UK PII: S0953-4075(00)50122-9

LETTER TO THE EDITOR

Electron scattering in cooled HCl: boomerang structures and outer-well resonances in elastic and vibrational excitation cross sections

Michael Allan†, Martin Čížek‡, Jiří Horáček† and Wolfgang Domcke§

† Institute of Physical Chemistry, University of Fribourg, Pérolles, CH-1700 Fribourg, Switzerland

‡ Department of Theoretical Physics, Faculty of Mathematics and Physics, Charles University Prague, V Holešovičkách 2, 180 00 Praha 8, Czech Republic

§ Institute of Physical and Theoretical Chemistry, Technical University of Munich, D-85747 Garching, Germany

Received 14 January 2000

Abstract. Differential cross sections for elastic scattering and excitation of the $v = 1$ vibrational level have been measured for rotationally cooled HCl at energies near the threshold for dissociative attachment. The cooling improves the visibility of the oscillatory structure in the $v = 0 \rightarrow 1$ cross section and permits the observation of a similar structure also in the elastic channel. The integral $v = 0 \rightarrow 1$ cross section and the resonant part of the integral elastic cross section have been calculated using a nonlocal resonance model. A high degree of agreement of the details of the measured and calculated structures confirms the correctness of the model and the high accuracy of the *ab initio* HCl^- potential-energy function used as input to the model.

The interest in the vibrational excitation cross sections in HCl has been initiated by the discovery of surprising threshold peaks by Rohr and Linder (1975, 1976). Narrow structures at thresholds for vibrational excitation appeared both in the inelastic cross sections of Rohr and Linder and in the measurements of the derivative of the elastic cross section at 180° by Burrow (1974). A later discovery of oscillatory structure in the $v = 0 \rightarrow 1$ and $v = 0 \rightarrow 2$ vibrationally inelastic channels (Cvejanović and Jureta 1989, Cvejanović 1993) was also unexpected in view of the large autodetachment width of the σ^* resonance. A number of theoretical and experimental studies on HCl and HF followed these discoveries. A complete list of citations would be too lengthy for this letter; examples are Rädle *et al* (1989), Knoth *et al* (1989a), Ehrhardt (1990), Schafer and Allan (1991) for the experiments, Dubé and Herzenberg (1977), Domcke (1990), Morgan *et al* (1990), Pleß *et al* (1992) and Fabrikant *et al* (1991) for theory. A nonlocal resonance model with variable threshold exponent and high quality resonant potential surface has recently succeeded in correctly describing both the threshold peaks and the oscillatory structures in the vibrationally inelastic channels, as well as dissociative attachment and associative detachment (Čížek *et al* 1999, Horáček 1999). A more comprehensive account of the entire subject and additional citations can be found in these two papers.

The energies of the structures found in the vibrationally inelastic cross section below the dissociative attachment threshold shift substantially with initial rotational quantum of the target HCl molecule (Čížek *et al* 1999). The experimentally observed structures are consequently strongly broadened by thermal rotational excitation at room temperature. We present here new

0953-4075/00/060209+05$30.00

measurements of the $v = 0 \rightarrow 1$ and the elastic channels, where the visibility of the structure is improved by cooling the sample HCl in a free jet expansion. The new experimental results are compared with the theoretical cross section of Čížek *et al* (1999) for the $v = 1$ channel and with new theoretical data for the elastic channel, calculated with the same model.

The measurements were performed using a spectrometer with hemispherical analysers described by Allan (1992 and 1995). Neat HCl was expanded from a 30 μm orifice, with a backing pressure of about one bar. Pronounced narrowing of the HCl elastic energy-loss peak with increasing backing pressure indicated significant cooling, although the exact temperature was not known. The analyser response function was determined on the elastic scattering in helium. The resolution of the instrument in the energy-loss mode (determined on the elastic peak of helium) was slightly below 20 meV fwhm, corresponding to an energy spread of about 14 meV in the incident beam. The energy of the incident beam was calibrated on the 19.366 eV ^{2}S resonance in helium and is accurate to within $\pm$30 meV. The excitation functions have been recorded at the maxima of the energy-loss peaks and emphasize consequently the $\Delta J = 0$ transitions.

The basic equation of the nonlocal resonance theory (Bardsley 1968, Domcke 1991) is the wave equation describing nuclear motion in the short-lived anion state

$$[T_{\mathrm{N}} + V_{\mathrm{d}}(R) - E]\psi_{\mathrm{d}}(R) + \int k\,\mathrm{d}k\,\mathrm{d}\Omega_k \int \mathrm{d}R' V_{\mathrm{d}\boldsymbol{k}}(R) G_0(R, R'; E - k^2/2) V^*_{\mathrm{d}\boldsymbol{k}}(R')\psi_{\mathrm{d}}(R') = -V_{\mathrm{d}\boldsymbol{k}_i}(R)\chi_{v_{\mathrm{i}}}(R) \tag{1}$$

with

$$G_0(R, R'; E) = \langle R|(E - T_{\mathrm{N}} - V_0 + \mathrm{i}\eta)^{-1}|R'\rangle. \tag{2}$$

Here R is the internuclear distance and $V_0(R)$ and $V_{\mathrm{d}}(R)$ are the potential energy functions of the target state and the discrete resonance state, respectively. $V_{\mathrm{d}\boldsymbol{k}}(R)$ denotes the discrete-continuum coupling matrix element. $\chi_{v_{\mathrm{i}}}(R)$ is the wavefunction of the initial vibrational state of the target molecule, $\boldsymbol{k}_{\mathrm{i}}$ the momentum of the incoming electron and E the total energy of the collision complex. G_0 is the Green's function for nuclear motion in the target state, T_{N} being the radial nuclear kinetic-energy operator.

From the solution of equation (1), the integral cross section for electron scattering from initial vibrational state v_{i} to final state v_{f} is obtained as

$$\sigma_{v_{\mathrm{f}}v_{\mathrm{i}}}(E) = \frac{4\pi^3}{k_{\mathrm{i}}^2} \int \mathrm{d}\Omega_{k_{\mathrm{f}}} \int \mathrm{d}\Omega_{k_{\mathrm{i}}} |\langle \chi_{v_{\mathrm{f}}}|V^*_{\mathrm{d}\boldsymbol{k}_{\mathrm{f}}}|\psi_{\mathrm{d}}\rangle|^2. \tag{3}$$

Expression (3) includes only the resonant part of the scattering amplitude, which is dominant for inelastic processes. For the elastic cross section, interference of the resonant amplitude with a background scattering amplitude has to be taken into account.

A more detailed discussion of the nonlocal formalism can be found in Domcke (1991). An improved nonlocal resonance model for the e + HCl system has been published recently (Čížek *et al* 1999). The calculations presented in the present work are based on this model (referred to as DMHC2 model in Čížek *et al* 1999). The parameters characterizing the functions $V_{\mathrm{d}}(R)$ and $V_{\mathrm{d}\boldsymbol{k}}(R)$ have been determined from fixed-nuclei *ab initio* electron-HCl scattering calculations (Padial and Norcross 1984) and high-level *ab initio* calculations for the bound part of the HCl^- potential energy function (Åstrand and Karlström 1990). The model thus contains no parameters which are adjusted to experiment.

The differential elastic cross section is compared with the calculated resonant part of the integral elastic cross section in figure 1. The cusp at the $v = 1$ threshold has already been observed by Knoth *et al* (1989b), who measured the elastic differential cross section in the energy range 0.15–0.6 eV, scattering angles of 60°, 90° and 135°, and a target HCl temperature

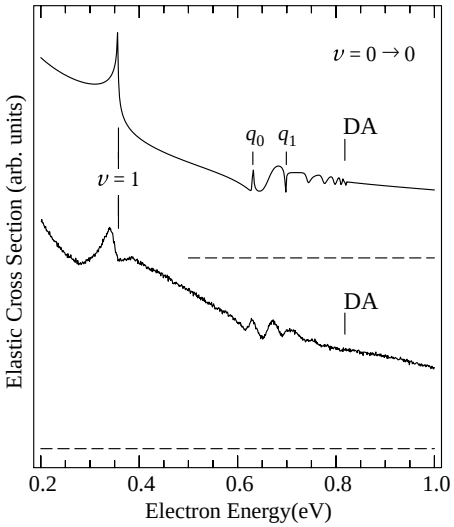

Figure 1. Experimental relative elastic cross section recorded at 90° (bottom) and calculated resonant part of the elastic cross section (top). Threshold for excitation of $v = 1$ and for dissociative attachment (DA) are marked. The symbols q_0 and q_1 are explained in the text.

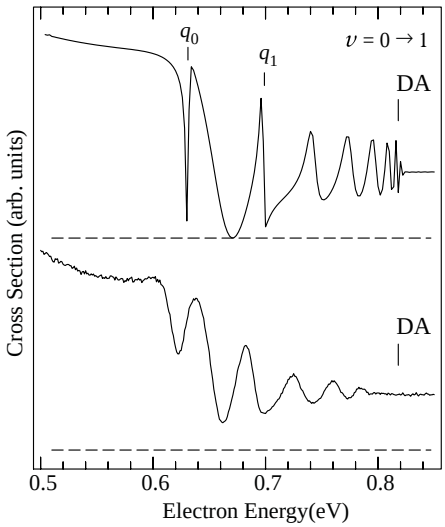

Figure 2. Experimental (differential, at 90°, bottom) and calculated (integral, top) cross section in the energy range where oscillatory structures are found. (see also caption of figure 1).

of 120 °C. The cusp appears more pronounced in the present curve, presumably due to the lower target temperature.

The present calculation assumes s-wave scattering and consequently isotropic behaviour of the resonant part. Rohr and Linder (1975) and Rädle *et al* (1989) found the experimental elastic cross section (at 3 eV) to be strongly forward peaked, as expected for a polar target, but the role of 'direct' scattering by the dipole moment of the target decreases with increasing scattering angle, justifying the present comparison. The shapes of the two curves in figure 1 agree very well. Both the pronounced cusp structure at the opening of the $v = 1$ channel and the oscillatory structure below the dissociative attachment threshold are well reproduced by the theory. The resolution of the present experiment is, however, not sufficient to confirm conclusively the very narrow width of the structures q_0 and q_1 in the calculated cross section (a peak at 0.63 eV and a dip at 0.70 eV).

Very good agreement is also found between experiment and theory for the $v = 0 \rightarrow 1$ cross section shown in figure 2. The comparison is more direct here because Rohr and Linder (1975, 1976) found an isotropic distribution of the vibrationally inelastic electrons at 2 eV (the σ^* resonance region), and the experimental differential and the theoretical integral cross sections thus should have the same shape. (Rädle *et al* (1989) and Knoth *et al* (1989) reported that the height of the threshold peak depends on scattering angle, but the threshold peak is not discussed in this letter.)

Similarly to the elastic cross section, the $v = 0 \rightarrow 1$ cross section has two very narrow features, marked q_0 and q_1 in figure 2 (essentially a dip at 0.63 eV and a sharp peak at 0.70 eV). The resolution of the instrument is comparable to the width of the structure and evidence for the narrow and wide structures may not be apparent at first glance. A closer look at the experimental curve does reveal evidence for the the narrow structures, however. The first 'valley', at 0.622 eV in the experiment, is 14 meV wide (full width at half depth), a width about equal to the energy spread in the incident beam, indicating a very narrow natural width

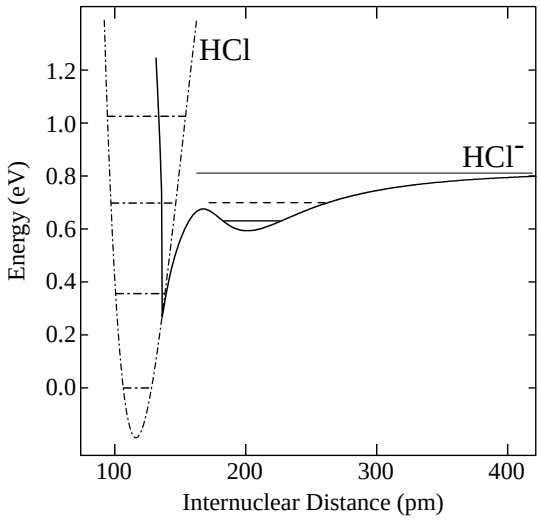

Figure 3. Potential curves of HCl (with vibrational levels) and HCl^-, taken from the publication of Čížek *et al* (1999). Energies of the sharp structures q_0 and q_1 are marked by a heavy solid and a dashed line, resp., and the threshold of dissociative attachment by a thin line.

of this dip. The second valley, at 0.661 eV in the experiment, is 22 meV wide, consistent with a natural width larger than that of the first valley. Evidence for the second sharp feature, q_2, can be derived from the shapes of the valleys. A consequence of this sharp feature is an asymmetrical shape of the third valley (at 0.72 eV) in the theoretical cross section. Its left flank is very steep, but its right flank rises only slowly, in contrast to the second valley which is essentially symmetrical, with flanks on both sides having about the same slope. The same characteristics are observed in the experimental spectrum: the valley at 0.66 eV is symmetrical, whereas the cross section in the next valley (at 0.70 eV) rises steeply on the left and more gradually on the right.

The relevant potential surfaces, taken from the paper of Čížek *et al* (1999), are shown in figure 3. The HCl potential curve is a Morse curve fitted to the true HCl potential curve. The HCl^- potential curve beyond the stabilization point is a parametrized fit to the *ab initio* results of Åstrand and Karlström (1990). A heuristically useful way to view the structures is interpreting the broader undulatory structure as being of 'boomerang' origin (a consequence of an interference between an outgoing and a reflected nuclear wave, see Herzenberg (1984)), and the superimposed very narrow structure q_0 as being a consequence of a quasibound vibrational level in the secondary minimum of the HCl^- potential curve at large R. The narrow width of q_0 is explained by the weakness of the coupling between the quasibound vibrational level in the outer well (*via* tunnelling) and the nuclear dynamics at shorter R. (This interpretation is less useful for the second structure, q_1, because it is already slightly above the potential barrier.) The narrow structure q_0 thus bears information on the shape of the HCl^- potential curve at large R. The good agreement of the observed and calculated energies of this structure (0.628 ± 0.03 eV and 0.631 eV, resp.) provides a confirmation of the accuracy of the *ab initio* calculation.

This research is part of project No 20-53568.98 of the Swiss National Science Foundation.

References

Allan M 1992 *J. Phys. B: At. Mol. Opt. Phys.* **25** 1559

——1995 *J. Phys. B: At. Mol. Opt. Phys.* **28** 5163

Åstrand P O and Karlström G 1990 *Chem. Phys. Lett.* **175** 624

Bardsley J N 1968 *J. Phys. B: At. Mol. Phys.* **1** 349

Burrow P D 1974 *J. Phys. B: At. Mol. Phys.* **7** L385

Čížek M, Horáček J and Domcke W 1999 *Phys. Rev.* A **60** 2873

Cvejanović S 1993 *The Physics of Electronic and Atomic Collisions: 18th ICPEAC (Aarhus) (AIP Conf. Proc. vol 295)* ed T Andersen *et al* (New York: AIP) p 390

Cvejanović S and Jureta J 1989 *3rd Eur. Conf. on Atomic and Molec. Phys. (Bordeaux)* Abstracts p 638

Domcke W 1990 *Aspects of Electron-Molecule Scattering and Photoionization (AIP Conf. Proc. vol 204)* ed A Herzenberg (New York: AIP) p 169

——1991 *Phys. Rep.* **208** 97

Dubé L and Herzenberg A 1977 *Phys. Rev. Lett.* **38** 820

Ehrhardt H 1990 *Aspects of Electron-Molecule Scattering and Photoionization (AIP Conf. Proc. vol 204)* ed A Herzenberg (New York: AIP) p 145

Fabrikant I I, Kalin S A and Kazansky A K 1991 *J. Chem. Phys.* **95** 4966

Herzenberg A 1984 *Electron-Molecule Scattering and Photoionization* ed P G Burke and J B West (New York: Plenum) p 187

Horáček J 2000 Inelastic low-energy electron collisions with hydrogen halides *The Physics of Electronic and Atomic Collisions* ed Y Itikawa *et al* (New York: AIP) p 329

Knoth G, Gote M, Rädle M, Leber F, Jung K and Ehrhardt H 1989a *J. Phys. B: At. Mol. Opt. Phys.* **22** 2797

Knoth G, Rädle M, Gote M, Ehrhardt H and Jung K 1989b *J. Phys. B: At. Mol. Opt. Phys.* **22** 299

Morgan L A, Burke P G and Gillan C J 1990 *J. Phys. B: At. Mol. Opt. Phys.* **23** 99

Padial N T and Norcross D W 1984 *Phys. Rev.* A **29** 1590

Pleß V, Nestmann B M, Krumbach V and Peyerimhoff S D 1992 *J. Phys. B: At. Mol. Opt. Phys.* **25** 2089

Rädle M, Knoth G, Jung K and Ehrhardt H 1989 *J. Phys. B: At. Mol. Opt. Phys.* **22** 1455

Rohr K and Linder F 1975 *J. Phys. B: At. Mol. Phys.* **8** L200

——1976 *J. Phys. B: At. Mol. Phys.* **9** 2521

Schafer O and Allan M 1991 *J. Phys. B: At. Mol. Opt. Phys.* **24** 3069